Compendium of Single Event Effects Test Results for Commercial Off-The-Shelf and Standard Electronics for Low Earth Orbit and Deep Space Applications

Brandon D. Reddell, Charles R. Bailey, Patrick M. O'Neill, Kyson V. Nguyen, Razvan Gaza, Chirag Patel, Jaime Cooper, Theodore Kalb, Elden Beach and Larry Mason

Abstract—**We present the results of Single Event Effects (SEE) testing with high energy protons and with low and high energy heavy ions for electrical components considered for Low Earth Orbit (LEO) and for deep space applications.**

I. Introduction

As NASA continues to operate the International Space Station (ISS) in Low Earth Orbit (LEO), it is facilitating the commercialization of LEO by working with companies through the Commercial Crew Program. Relevant to the design and operation of hardware in this environment, there is a need to select electronic components that are known to function for various mission durations. The environments here are relatively benign with occasional passes through the South Atlantic Anomaly region of the trapped proton Van Allen belt. Certification has primarily been carried out through high energy proton testing, which has been successfully used to test for Single Event Effects (SEE) in LEO for over two decades in the Space Shuttle and ISS programs [1]-[2]. It is anticipated that high energy protons will continue to be used by companies intending to fly short duration programs in LEO.

The new focus of the human space exploration program at NASA is focused on destinations in cis-lunar space and eventually to Mars with the Orion Multi-purpose Crew Vehicle being developed by the Lockheed Martin Corporation. Additionally, smaller-scale projects such as small satellites, robotic rovers, and various science payloads will be exposed to similar environments. For all of these missions, the hardware will be exposed to Galactic Cosmic Radiation (GCR) and possibly Solar Particle Events (SPE). SPEs are primarily proton events, but contain concentrations of heavy ions, whereas GCR are heavy ions ranging from hydrogen through iron spanning many orders of magnitude in energy. For these missions, program performance and reliability requirements necessitate the need for heavy ion certification. To date, this has been carried out by traditional (low energy) heavy ion testing as well as using the Variable Depth Bragg Peak (VDBP) method for part characterization and for destructive screening.

NASA has primarily conducted proton testing at the Indiana Cyclotron Facility until closure in December 2014, and afterwards, at the Francis Burr Proton Facility (FBPTC) in Boston, Ma. For heavy ions, NASA continues to use Lawrence Berkeley National Laboratory (LBNL) and the Texas A&M Cyclotron Facility (TAMU) for low energy testing. For high energy testing, NASA has been using the techniques developed by the NASA Johnson Space Center to use the high energy beams at Brookhaven National Laboratory at the NASA Space Radiation Laboratory [3]-[5].

This paper summarizes the test results through the year 2016 in the above mentioned programs and provides generic information to allow the user to evaluate radiation performance for various radiation environments.

II. TEST PROTOCOL

A. Proton testing

NASA uses 200 MeV protons to test for destructive and nondestructive errors for hardware intended for LEO, i.e. for the International Space Station (ISS) [6]-[7]. This test exposes most known failure modes that have a Mean Time Before Failure (MTBF) <= 10 years in the LEO environment. Proton testing replicates approximately 6-10 years of the heavy ion linear energy transfer (LET) environment up to an LET of approximately 10-14 MeV-cm^2/mg in silicon. The proton beam typically loses less than 10% of its energy while passing through the electronic parts. Secondary recoils are typically produced though the inelastic collisions of individual protons with the nuclei in the device, which is primarily silicon, but may contain higher charge elements such as tungsten.

B. D. Reddell, C. R. Bailey, P. M. O'Neill, and K. V. Nguyen are with the NASA Johnson Space Center, Electronic Design and Manufacturing Branch, 2101 NASA Parkway, Houston, Texas 77058.

(email: brandon.d.reddell@nasa.gov, charles.r.bailey@nasa.gov, patrick.m.oneill@nasa.gov, and Kyson.v.nguyen@nasa.gov)

R. Gaza, C. Patel, J. Cooper, T. Kalb, E. Beach and L. Mason are with Lockheed Martin Space Systems Company, Houston, Texas, 77058.
(email: razvan.gaza@lmco.com, chirag.patel@lmco.com, jaime.cooper@lmco.com, theodore.kalb@lmco.com, elden.beach@lmco.com, and larry.mason@lmco.com.

The typical test exposes the device under test to a fluence of $\geq$ 1E+10 protons/cm2 which accomplishes two goals. The first is to find single event effects caused by heavy ions up to LET of ~10 MeV-cm^2/mg. Secondly, the test produces a total ionizing dose (TID) of at least 600 rads (Si), which corresponds to about 10 years of total ionizing dose exposure in LEO.

This NASA method does not fully characterize the part, but it intends to screen for hard failures and provides very conservative estimates up to a 10 year MTBF in LEO [6]-[8]. This test is typically performed at the board or box level which provides a means to reduce the cost of testing, especially with modern Commercial Off-The-Shelf (COTS) units. The test can be used for down-selection for both LEO and deep space applications as well as provide conservative SEE and TID results.

B. Traditional Heavy Ion Testing

NASA uses traditional methods to perform heavy ion testing and requires each part be characterized to high LET (depending on mission) or failure. Traditional methods require delidding of the parts for single piece part testing and characterization. Often times, components with specific application voltages representative of flight like conditions are tested to understand transient radiation induced responses to these devices or test for the effectiveness of mitigation strategies. Analyses of the SEE signatures at the system level are required to determine the system effects and what mitigations are necessary. Testing complex parts and applying those results to complex systems is a difficult task. The radiation analysis typically involves circuit analysis to evaluate the system level effects while cataloging the effects of each part in the system.

C. High Energy Heavy Ion Testing

Increasingly, the human rated missions are incorporating complex parts that are too difficult (or costly) to delid or have sensitive volume depths unreachable by low energy heavy ion beams. This problem has been encountered on the Orion Multipurpose Crewed Vehicle program [9]. Additionally, designs include more Commercial Off-The-Shelf (COTS) units to support crew activities for which there are no rad-hard versions available. In these cases, the traditional test facilities at TAMU and LBNL cannot provide beams with enough energy to penetrate these devices. Furthermore, NASA JSC is seeing a trend towards screening flight boards to certain LET levels for destructive effects while also using the high energy beams to evaluate flight circuits for evaluation of system level soft errors. For individual parts characterization, we implore the Variable Depth Bragg Peak (VDBP) method [3]-[5] and for screening, a modified VDBP method which uses the various degrader steps to ensure all locations in the board are exposed to a certain LET level desired by the program. All VDBP testing reported in this report was accomplished using the ion beams listed in Table 1. The NSRL staff have published an overview of the NSRL facility with more details on beam ion selection and other beam characteristics [10].

Table 1
LET (Si) for Ion Beams Used For VDBP Testing

	Max Energy (MeV/n)	LET at Max E (MeV-cm2/mg)	Peak LET (MeV-cm2/mg)**	Range in Si (mm)
H^1	2500	0.00171	0.51	5470
C^{12}	1500	0.06227	5.2	972
Fe^{56}	1470	1.171	29.3	235
Kr^{84}	383	3.28	41	26.5
Xe^{132}	350	7.7	69.2	16.3
Ta^{181}	342	14.8	87.5	12.1
Au^{197}	165	24.7	94.2	3.7

* This table was reproduced from the official listing at https://www.bnl.gov/nsrl/userguide/beam-ion-species-and-energies.php
**This represents the Peak LET of a single particle. The average LET of will be lower because of the energy spread of the beam, and this depends on energy.

For VDBP destructive screening, a series of degrader steps are used to slide the Bragg curve through the whole device. Where the Bragg curves intersect will define a minimum LET exposure at all locations in that device and this value is a function of the degrader step size used. Figure 1 shows the 165 MeV/n Au beam with 0.3 mm of degrader will expose the whole part to an LET of 69 MeV-cm2/mg or higher.
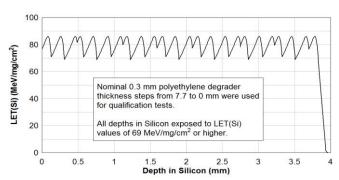

Fig. 1. Example of destructive screening with 165 MeV/n Au ion with 0.3 mm steps of polyethylene degrader. A part with 3.5 mm of Si (equivalent) will be exposed to a minimum of LET=69 MeV-cm^2/mg.

III. TEST RESULTS OVERVIEW

Table 2 is an excerpt from the testing results table that includes over 100 parts. For each part, the table gives the report number, the part number, the Lot Date Code (LDC), part type, manufacturer, where it was tested and to what LET and characterization data when determined, i.e. a set of Weibull parameters for heavy ion data and Bendel parameter for proton test data, along with important notes. The LDC's are provided for the tested parts because part manufacturing variations are known to affect radiation susceptibility and this information is

Table 2: Summary of SEE Test Results					
Part #	**LDC**	**Part type**	**Manufacturer**	**Facility**	**Weibull Parameters**
OLF300	504	Opto	Iso Link	TAMU	σ_0=1.4E-4, Max SET=450mV, Max LET=80.2
RH1499	1002A	Quad opamp	AD	TAMU	L_0=15, σ_0=8.5E-3, W=19, S=1.4, SET pos=2us, ,2V, SET neg = 0, Max LET=80.2
REF02	1025A	Volt Reg	AD	LBNL	No SET above 6V, Vsup=15, Vout=5V, Max LET=75.7
RH1016MW	1011A	High Speed Comp	LT	LBNL	L_0=12.5, σ_0=6E-5, W=50, S=2.5, SET= +/- 0.5V, Max LET=75.7
SNV54AHC244W	0726A	Octal buffer	TI	LBNL	No SET between 1.3V and 0.8V. Operating at 3.3V, No DSEE, Max LET=75.7
HYSE-117RH-Q	Proto – same as flight	Adj Pos volt reg	Intersil	LBNL	L_0=7, σ_0 =1.2E-4, W=40, S=3
OLI249	114814	Opto	Isolink	LBNL	L_0=25, σ_0 =6.0E-3, W=50, S=4, SET>= 2.2V,Vsup and Vout=3.3V, 60us duration maximum, Max LET=75.7
RH1014MW	1101A	Quad op amp	LT	TAMU	L_0=8.6, σ_0 =8.4E-4, W=32, S=3, Max POS SET=8V/22us L_0=1.8, σ_0 =7.0E-3, W=26, S=1.7, Max NEG SET=-9V/60us, Max LET=87.1
LMC6484	1043	Quad op amp	National Semiconductor	TAMU	No SEL, SET < 10us, Max LET=87.1
HS-4423BRH	X1006A	Dual Inv MOSFET Driver	Intersil	TAMU	L_0 = 19, σ_0 = 2.94E-05, W = 16.03, S=1.926, 80nS transients, Max LET=85.4
54LVC08A	1217A	Quadruple 2-input AND Gate	TI	IUCF	200 MeV, 1E10/cm^2
SG7805AT	7C1143P	5V Voltage Regulator	Microsemi	IUCF	200 MeV, 5E10/cm^2
IS705RH	1113AC	Power-up/down Microprocessor Reset Circuit	Intersil	NSRL	SET: σ_0=7.47E-5, L_0=22, W=26.85, s=3.09, No SEL to LET=60 with 1E6/cm^2
IRHM7360SE	542	400V N-Channel MOSFET	International Rectifier	TAMU	176V at 40 LET pass voltage (9KOhm load)
IRHF7330SE	918	400V N-Channel MOSFET	International Rectifier	TAMU	Pass at 182V at LET =40, (shorted output)
SCF128XFTG64C	1201	128M NV Flash ROM	Xilinx	IUCF	No switched bits
IRHY57230CMSE	1110	200V N-Channel MOSFET	International Rectifier	TAMU	Pass at 182V at LET= 85.4, (shorted output)
66099	1046	Optocoupler	Micropac	IUCF	Bendel FIT A=15.48 (single point)
66252	1219	Optocoupler	Micropac	IUCF	No SET observed, 15V and 3.3V bias
UC1845	0910A	PWM	TI	LBNL	L_0=3, σ_0 =2.0E-3, W=28, S=1.3, SET at +/- 50% duty cycle, Max LET=75.66
SNV54AC14W-SP	1131A	Hex inverter, Schmidt tr.	IR	TAMU	SET Lo >39.9, Low-high SET from ground to rail (3.3) at LET=85.4,
AD589	231	Volt Reference	AD	LBNL	SET1: Short positive (less than 50ns) followed by 8uS negative 400mV Weibull: L_0=2, σ_0 =4.0E-4, W=2, S=1.1 SET 2: 1us, 500mV. Weibull: L_0=24, σ_0 =2.0E-4, W=20, S=1, both tested at LET=75, No DSEE
OP27	145	Op-amp	AD	LBNL	SET1: 1V, 150uS. Weibull: L_0=3.4, σ_0 =8.0E-4, W=15, S=2

Part	Lot	Device Type	Manufacturer	Facility	Comments
					SET2: -500mV, 150uS. Weibull: $L_0=25$, $\sigma_0=1.0E-4$, W=20, S=4, 12V bias, output=2V, No DSEE, Max LET=75.6
66260-300	1104	Optocoupler	Micropac	LBNL	Vcc=3.3V SET: 1V, 40us Weibull: $L_0=3.2$, $\sigma_0=2.0E-3$, W=20, S=12, Max LET=75.6
66252-000	707	Optocoupler	Micropac	LBNL	Vcc=3.3V, SET: -3.3V, 400ns Weibull: $L_0=9.5$, $\sigma_0=2.0E-4$, W=14, S=1.9, Max LET=60
ILD2	V937H	Optocoupler	Vishay	LNBL	SET1: -3V, 40us Weibull: $L_0=9.5$, $\sigma_0=1.6E-3$, W=20, S=2 SET2: -2V, 200ns Weibull: $L_0=3$, $\sigma_0=4.0E-4$, W=8, S=1.2, Max LET=60
HS-4423	**	FET driver	Intersil	LNBL	No SET, Bias at 13V, Max LET=75.7
VRG8662	1002	LDO reg	Aeroflex	TAMU	SET at high LET (56>SET>=87.1), No DSEE
IS-1009RH	451	2.5V Reference	Intersil	TAMU	Vsupply=13V, Vout=2.5V SET1: 0.5, -2V, 5us. Weibull: $L_0=5.7$, $\sigma_0=8.1E-4$, W=14.6, S=1 SET2: same as 1 but 45us. Weibull: $L_0=5$, $\sigma_0=7.4E-5$, W=17.7, S=1.226, No DSEE, Max LET=87.1
66266	1119	Optocoupler	Micropac	TAMU	SET: -700mV to 1.1V (from Vout), 50-70us, Weibull: $L_0=1$, $\sigma_0=2.9E-3$, W=21.4, S=5, Vout=15V, Max LET=60
IRHLG77214	1126	250V Quad N-Channel MOSFET	IR	TAMU	No SEB at 182V at LET= 87.1, gate leakage noted on 2 units
IS-1009RH	451	Linear bipolar	Intersil	TAMU	SET: Pos: 600mV/ 1.5us Neg: -1.75V/ 19us, No SEL, Max LET=77.3
OLF-300	504	Optocoupler	Isolink	TAMU	All transients below 3V, Max LET=77.3
GoPro Hero 3	**	Camera	GoPro		Camera survived with many SEE
MKD25PA128IO-672A	**	Solid State Drive Assy	Memkor	IUCF	DSEE: Unit failed to respond to power cycle. Bendel A = 13.08
IRHF7330SE	1406	N-Channel MOSFET	IR	TAMU	Degradation observed at 1E5, Max LET 77.3
IR2110L4	1146	FET driver	IR	TAMU	SET: State changes and transients, No DSEE, Max LET=77.3
HERO4		Camera	GoPro	IUCF	Numerous SEE, no DSEE
IRHQ57214SE	1436	250V N-Channel MOSFET	IR	TAMU	Pass at Vds=171V, LET=77.3. SET=+/-4V on the drain, +/- 1.75V on the source. <0.5us duration
DFI downselect: NSW-5FT-TGE-2, Ethos Lite, X52000001-01, X92000001-01	**	5 Port Switch	TTC	IUCF	No DSEE after $1E10/cm^2$
IRHF7110SCS	1130	100V, N-Channel MOSFET	IR	TAMU	Vds=20V, no DSEE or degradation.

IRHYS67234T3	1439	250V, N-Channel MOSFET	IR	TAMU	Vds=240V, No DSEE or degradation.
2N3439	1148	350V, NPN BJT	Microsemi	TAMU	SET=1.8V/<0.5us, σ_0 = 2.33E-3 Vce=166V, No DSEE
OP27AL	0936A	Linear Bipolar	AD	LBNL	DSEE: Above LET=45.6
Hero3	**	Camera and associated electronics	GoPro	NSRL	DSEE at LET=4.2
MACQ-500E-2	**	Overhead module	TTC	FBPTC	Unit failed in less than 1E10/cm2
RH1013MW	1320A	Precision Op-amp	Linear Technology	LBNL	largest SET: 5.7V, 13 usec, No DSEE
OP484	1009A	Op-amp	AD	LBNL	No SEDR. Trigger >250mV, 1V/1uS max transient, Weibull: L_0=0.1, σ_0 =2.8E-3, W=37, S=3, Vcc=17.7V
900613	**	SSD	VisionTek	NSRL	DSEE: σ_0=1.12E-6 at LET=>4.2 (upper limit)
KVR16LS11/4	**	DRAM	Kingston	NSRL	DSEE: σ_0=4.5E-7 at LET=>4.2 (upper limit)
IRHF7110SCS	1130	N-Channel 100V MOSFET	International Rectifier	TAMU	No DSEE or degradation, Vds=20V Max LET=75
88E1111-NDC2	1307	PHY	Marvell	TAMU	SEU "Packet Errors" Weibull: L0=0.1, σ_0 =1.3E-3, W=70, S=1.3 SEFI Weibull: L0=0.1, σ_0 =9.0E-6, W=70, S=0.7, cleared with RESET or power cycle Max LET=77
WIL6120	**	Radio controller	Wilocity	NSRL	SEE σ_0 =3.65E-4 at LET=>4.2 (upper limit for self-recovering SEE) SEE σ_0=5.58E-4 at LET=>4.2 (upper limit for SEE requiring intervention)
NSW-12GT-1	**	12 bit Ethernet Switch	TTC	MGH	SEFI requiring power cycle: Bendel A=13.07 DSEE: Bendel A=18.03
SN54AC14W	1131A	Hex inverter/Schmitt trigger	TI	LBNL	SET=+/-200mV, No SET at 48.2 Upper limit σ_0=3.85E-6 at LET=75.6
NSW-12GT-1 (power supply only)	**	28V to 5V converter	TTC	NSRL	DSEE σ_0=1.00E-5 at LET=>14.2 (upper limit)
Hero4 Black	**	Portable HD Digital Video Camera	GoPro	NSRL	DSEE σ_0=1.36E-6 at LET=>14.2 (upper limit)
D54250WYK1	**	SBC	NUC Intel	NSRL	DSEE σ_0 =9.04E-5 at LET=>14.2 (upper limit)
MAGBES-21HS	**	5 Port Ethernet Switch	MPLAG Elektronikunternehmen	NSRL	DSEE σ_0=1.87E-6 at LET=>14.2 (upper limit)
PIP37-1	**	Ruggedized SBC	MPLAG Elektronikunternehmen	NSRL	DSEE σ_0=5.06E-4 at LET=>14.2 (upper limit)
GoPro Htr 6/8/2015 DSS	**	Heater board	Deep Space Systems	NSRL	DSEE σ_0=5.05E-7 at LET=>14.2 (upper limit)
NSW-8GT-TG-D-1	**	8 Port Network Switch	TTC	MGH	SEE: Bendel A=14.81
175-0600-0103L	**	5 Port Ethernet Switch	Gadget Smyth	MGH	SEE Bendel A=12.73 (self-recovering SEE) SEE Bendel A=14.33 (SEE requiring intervention) DSEE: Bendel A=15.01
ATXMEGA128A1U	1504	Microcontroller	Atmel	TAMU	Stuck bits – stuck at 0. Weibull: L_0=16.2, σ_0=7.9E-5, W=101.3, S=2.3

					tested powered to LET=77
66183	**	OptoCoupler	Microsemi	NSRL	No SEE noted, using VDBP method
JANSF2N7484T3	**	MOSFET	IR	NSRL	No SEE noted, using VDBP method
QT625LBM-25.8 MHZ	**	Oscillator	Q-Tech	NSRL	SEFI: Weibull: L_0=1.0, σ_0=7.9E-6, W=5.9, S=5.01 Max LET=60+ using VDBP method
IS9-139ASRH	**	Voltage Comparitor	Intersil	NSRL	No DSEE to LET=60+
IS9-1825ASRH	**	PWM Controller	Intersil	NSRL	No DSEE to LET=60+
SPT6235M-NPN	**	Transistor	SSDI	NSRL	No SEE noted to LET=60+ using VDBP method
LMC6482A-HCI	**	Op Amp	Texas Instrument	TAMU	SETs application dependent
4011BEDIE2HR	**	NAND Gate	ST-Micro	LBNL	Worst case SET: -370 mV, 20 nsecs, Max LET=77.5
74HC02	1145	Quad 2-inout NOR Gate	Fairchild Semi	TAMU	No SETS, No DSEE
RIC7113A4SCS	1424	High/Low side Gate Driver	IR	TAMU	Longest Dropout 550 msecs, No DSEE, Max LET=77
74AC00	1507	Quad 2-inout NAND Gate	Fairchild Semi	LBNL	Worst SET =+/- 300 mV, 58 nsecs, No DSEE, Max LET=75
HCPL-523K #300	1314	Dual Logic Opto	Avago Technologies	LBNL	No DSEE, Max LET=75
OLH249	1548	Opto - Hybrid	Isolink	LBNL	Worst case SET: 1.28V, 70 usecs, Max LET=75
RH6105	**	Current Sense Amp	Linear Tech	LBNL	Worst case SET: 3V / -1V, < 9 usecs, Max LET=75
XCF128XFTG64C	99A3R VS, MYS 99 538	FLASH non-volatile Memory	Xilinx	NSRL	1 bit-flip was observed at LET ~ 40, VDBP method
SN54AHC244W	726	Octal Buffer	TI	TAMU	High Temp No DSEE, Max LET=77
IS42S16400J-5BL	**	SDRAM	ISSI	NSRL	Bitflip Error: Weibull: L_0=.01, σ_0 =4.6E-1, W=110, S=2.9 No DSEE: 7.68E4/cm^2 at LET=39.
SI7415DN-T1-GE3	**	P Channel MOSFET	Vishay	NSRL	No DSEE at LET=29, 12V
DS2411R+T&R	**	SCSI terminator	Maxim	NSRL	No DSEE for 7.79E4/cm^2 at LET=39
TMP006AIYZFR	**	Thermopile	TI	NSRL	Local temp error: Weibull: L_0=10, σ_0 =2.5E-5, W=14, S=4. Obj temp error: Weibull: L_0=5, σ_0 =5E-0, W=0.1, S=10. No DSEE: 7.37E4/cm^2 at LET=29.
74AUP1G157GW	**	Analog Mux	NXP	NSRL	No SEE at 1.61E5/cm^2 at LET=39
ASDMPC-10.000MHZ-RT-T	**	Oscillator	Abracon	NSRL	Failed immediately.
DS1339A	**	Clock	Maxim Integrated	NSRL	Soft Errors: Weibull: L_0=12, σ_0 =9E-5, W=0.1, S=10 No DSEE: 7.54E4/cm^2 at LET=29
SN74LVC1G66DCKR	**	Analog switch	TI	NSRL	No SEE, DSEE: 7.62E4/cm2 at LET=29
N25Q128	**	Flash memory	Micron	NSRL	Read Error: Weibull: L_0=1, σ_0 =4E-5, W=27, S=2 No DSEE: 7.5E4/cm^2 at LET=29
SN74CBTLV3257RSVR	**	Mux/demux and Bus switch	TI	NSRL	No SEE noted at 7.55E4/cm^2 DSEE: 7.55E4/cm^2 at LET=29
NC7SZ125M5X	**	Tri-state buffer	On Semiconductor	NSRL	No SEE noted. DSEE: 7.55E4/cm^2 at LET=29.
SN74AHC1G08DBVR	**	Quad AND Gate	TI	NSRL	No SEE noted. DSEE: 7.55E4/cm^2 at LET=29
SN74LVC1G125BDVR	**	Tri-state buffer		NSRL	No SEE or DSEE: 7.55E4/cm^2 at LET=29

CB3LV-3C-25MHZ	**	Oscillator		NSRL	No SEE at 7.55E4/cm^2 DSEE: 7.55E4/cm2 at LET=39
FDMC86139	**	P-Channel MOSFET, 100V	Fairchild/ON semi	NSRL	No DSEE for 1E5/cm^2 at LET=11.75
TLV70133	**	Linear Regulator	TI	NSRL	No DSEE for 1E5/cm^2 at LET=11.75
TPS22929	**	Single Load Switch	TI	NSRL	No DSEE for 1E5/cm^2 at LET=15
CB3LV	**	Oscillator	CTS-Frequency controls	NSRL	No DSEE for 1E5/cm^2 at LET=15
TPS73601	**	Linear Voltage Regulator	TI	NSRL	No DSEE for 1E5/cm^2 at LET=11.75
	**				
NAND Flash	**			NSRL	No DSEE for 1E5/cm^2 at LET=11.75
DP83640	**	Precision PHYTERTM IEEE 1588 Transceiver	TI	NSRL	No DSEE for 1E5/cm^2 at LET=11.75
OPA2209	**	Precision Op Amps	TI	NSRL	No DSEE for 1E5/cm^2 at LET=11.75
LM4040	**	Voltage Reference	ON-Semi	NSRL	No DSEE for 1E5/cm^2 at LET=11.75
LT3092	**	200mA 2-Terminal Programmable Current Source	Linear Technology	NSRL	No DSEE for 1E5/cm^2 at LET=11.75
OMAP L138	**	ARM/DSP Processor		NSRL	L2 Error: Weibull: L_0=1, σ_0 =2.23E-2, W=57, S=1.04 Overcurrent: L_0 = 24, σ_0=3E-4 L3 Error: Weibull: L_0=1, σ_0 =2.88E-4, W=16.6, S=1.166 L1D Error: Weibull: L_0=1, σ_0 =8.57E-3, W=120.8, S=1.2 CPU Functional Interrupt: Weibull: L_0=1, σ_0 =4.15E-4, W=55.2, S=1.2 PRU Functional Interrupt: Weibull: L_0=3, σ_0 =2E-4, W=0.1, S=10 Software error: Weibull: L_0=3, σ_0 =2.1E-4, W=19.5, S=1.628
FRO15L3EZ	**	Reverse Polarity Device	ON Semiconductor	NSRL	No DSEE: LET=39, 1E6/cm^2
TPS62142	**	Temperature Sensor	TI	NSRL	No DSEE: LET=39, 1E6/cm^2
TPS73601	**	Remote Power Regulator	TI	NSRL	No DSEE: LET=39, 1E6/cm^2
RM48L950	**	16/32 BIT RISC Flash Microcontroller	TI	NSRL	RAM single bit error: Weibull: L_0=3, σ_0 =1.44E-2, W=19.5, S=1.628 Software error: Weibull: L_0=1, σ_0 =2.1E-4, W=27.3, S=0.869 Flash error: Weibull: L_0=2.7, σ_0= 5.5E-4, SEFI: Weibull: L_0=1, σ_0 =6.0E-4 No DSEE: LET=39, 9E3/cm^2
KSZ8895	**	Ethernet Switch	Microchip Tech.	NSRL	DSEE: Weibull: L0=12, v =1.59E-3, W=5.4, S=2.376
MT29F32G08	**	NAND flash	Micron	NSRL	MTD2 Byte error : Weibull: L_0=3, σ_0 =1.3E-1, W=66.15, S=2.38. ECC was very effective at lower LET Erase Failed Error: Weibull: L_0=4, σ_0 =1.3E-4, W=23.8, S=0.462 MTD2 Bad Block Error: Weibull L_0=2, σ_0 =1.0E-4

					No DSEE: LET=51, 5E4/cm^2
NVH0505	**	DC/DC converter		NSRL	No DSEE to LET=51, 9E3/cm2
AD5622	**	Bias converter DAC	Analog Devices	NSRL	No SEE or DSEE at LET=24, 1E4/cm^2
AD7991	**	Bias converter ADC	Analog Devices	NSRL	No SEE or DSEE at LET=24, 1E4/cm^2
MAX9619	**	Remote Temp sensor	Maxim	NSRL	No SEE or DSEE at LET=24
AGLN250V2-VQG100	**	Flash FPGA	Microsemi	NSRL	SEFI: L$_0$=18, S0=3E-5 No DSEE to LET=51, 9E3/cm^2
MT46H64M16LFB	**	DDR memory	Micron	NSRL	Single bit error: Weibull: L$_0$=9, σ_0 =9E-3, W=10, S=1.274 Multiple bit error: Weibull: L$_0$=9, σ_0 =1E-4
LAN8710A-EZC	**	Ethernet PHY	Microchip Tech	NSRL	SEFI: L$_0$=2, σ_0=1E-4 No DSEE to LET=39, 1E4/cm^2
74LCX573	**	Octal Latch	Fairchild Semiconductor	NSRL	No SEE or DSEE at LET=24, 1E4/cm^2
DS90LV047/48	**	Quad Line Driver/receiver	TI	NSRL	No SEE or DSEE to LET=39
TIMEPIX	**	Radiation sensor	Timepix	NSRL	No SEE or DSEE to LET=39
MAX6692	**	Temp Sensor	Maxim	NSRL	No DSEE to LET=26.5
LTM4644IY	**	Quad switcher		NSRL	DSEE around LET=3
TPS54295RSAT	**	Switching Regulator	TI	NSRL	SEFI: Weibull: L$_0$=4, σ_0 =4.5E-5, W=3, S=2 DSEE at LET=19
LTC3646	**	Step down regulator	Linear Technology	NSRL	Trigger: Weibull: L$_0$=3, σ_0 =2.65E-4, W=44, S=1.38 SEFI: Weibull: L$_0$=39, σ_0 =9E-5 No DSEE to LET=39, 9E4/cm^2
LM3880Q	**	Power Sequencer	TI	NSRL	No SEE to LET=24, 9E3/cm^2 No DSEE to LET=39
INA230	**	Bidirectional current/power monitor	TI	NSRL	Trigger error: Weibull: L$_0$=24, σ_0 =7E-5, W=35, S=1 Register error: Weibull: L$_0$=24, σ_0 =6E-5, W=15, S=1
OMH3040 OMH3005S	1523	Hall-effect Sensor	TT Electronics / Optek	LBNL	Worst case SET: 15V to ground, 4 usecs, No DSEE at LET= 77.5
4011BEDIE2HR	**	NAND Gate	ST-Micro	LBNL	Worst case SET: -370 mV, 20 nsecs, No DSEE at LET=77
74HC02	1145	Quad 2-inout NOR Gate	Fairchild Semi	TAMU	No SET or DSEE at LET=77
RIC7113A4SCS	1424	High/Low side Gate Driver	IR	TAMU	Longest Dropout 550 msecs, No DSEE at 77
JANTXV2N3439UA	1447	High V Transistor	Microsemi	TAMU	Worst case SET: 2V and -2.4V, < 100 nsecs, No DSEE at LET=77
OMH3075	_0043	Hall-effect Sensor	TT Electronics / Optek	TAMU	Worst case SET: 15V to ground, 5 usecs, No DSEE at LET=75

useful when assessing current parts against previously tested parts.

I. Test Results and Discussion

In this section, details for individual tests are discussed to provide more information as required. Additionally, test results analyses are discussed. The usage of the 1-parameter Bendel curve is discussed along with the development of the Weibull parameters from the high energy heavy ion test. Specific details of the VDBP test results analyses are also discussed.

II. Conclusions

We have presented proton test data and/or heavy ion test data results for a variety of piece parts and/or COTS units being considered for applications in a LEO or deep space radiation environment. Additionally, test data from high energy heavy ion testing (VDBP) has been discussed and presented. As NASA continues to develop plans for deep space missions, new radiation-related challenges will exist with the increased use of COTS parts and hardware. With limited budgets, designers are increasingly looking to published data in compendiums such as this to help make decisions on parts.
.

III. Acknowledgment

We would like to thank the support staff at LBNL, TAMU, Francis Burr and other proton facilities for the professional and excellent support. Additionally, we are very thankful to Mike Sivertz and Adam Rusek of NSRL for the continued expertise in helping make Variable Depth Bragg Peak testing and screening a reality.

IV. References

[1] C. K. Kouba, K. V. Nguyen, P. M. O'Neill, and C. R. Bailey, "Proton Radiation Test Results on COTS-Based Electronic Devices for NASA-Johnson Space Center Spaceflight Projects", *2006 IEEE Radiation Effects Data Workshop*", Ponte Vedra Beach, Fl, 2006, pp. 26-36.

[2] K. K. Allums, P. M. O'Neill, B. D. Reddell, C. R. Bailey, K. V. Nguyen, "Radiation Test Results on COTS and Non-COTS Electronic Devices for NASA Johnson Space Center Spaceflight Projects", *2012 IEEE Radiation Effects Data Workshop*", Tucson, Az, 2012, pp. 1-9.

[3] S. Buchner, N. Kanyogoro, D. McMorrow, C.C. Foster, P. M. O'Neill and K. V. Nguyen, "Variable Depth Bragg Peak Method for Single Event Effects Testing" *IEEE Trans. on Nucl. Sci.*, vol. 58, no. 6, pp. 2976-2982, Dec. 2011.

[4] N. J. H. Roche et al., "Validation of the Variable Depth Bragg Peak Method for Single Event Latchup Testing Using Ion Beam Characterization" *IEEE Trans. on Nucl. Sci.*, vol. 61, no. 6, pp. 3061-3067, Dec. 2014.

[5] C. C. Foster, "Certification of Parts for Space With the Variable Depth Bragg Peak Method" *IEEE Trans. on Nucl. Sci.*, vol. 59, no. 6, pp. 2909-2913, Dec. 2012.

[6] P. M. O'Neill, G. D. Badhwar and W. X. Culpepper, "Risk assessment for heavy ions of parts tested with protons" *IEEE Trans. on Nucl. Sci.*, vol. 44, no. 6, pp. 2311-2314, Dec. 1997.

[7] P. M. O'Neill, G. D. Badhwar and W. X. Culpepper, "Internuclear cascade-evaporation model for LET spectra of 200 MeV protons used for parts testing" *IEEE Trans. on Nucl. Sci.*, vol. 45, no. 6, pp. 2467-2474, Dec. 1998.

[8] C. C. Foster, P. M. O'Neill and C. K. Kouba, "Risk Assessment Based on Upset Rates From High Energy Proton Tests and Monte Carlo Simulations" *IEEE Trans. on Nucl. Sci.*, vol. 55, no. 6, pp. 2962-2969, Dec. 2008.

[9] L. Hoffmann and V. Lam, "Qualification of an Automotive-Grade, State-of-the-Art ASIC for Natural Space Applications" *2013 IEEE Radiation Effects Data Workshop*", San Francisco, Ca., 2013, pp. 1-8.

[10] C. La Tessa, M. Sivertz, I. Chiang, D. Lowenstein and A. Rusek, "Overview of the NASA space radiation laboratory" *Life Sciences in Space Research,* vol. 11, pp. 18-23, Oct. 2016